J Neurophysiol 120: 2583–2594, 2018.
First published September 12, 2018; doi:10.1152/jn.00392.2018.

RESEARCH ARTICLE | *Control of Movement*

Cortico-cerebellar network involved in saccade adaptation

Alain Guillaume,[1,2] Jason R. Fuller,[2] Riju Srimal,[3] and Clayton E. Curtis[2,3]
[1]*CNRS, Laboratoire de Neurosciences Cognitives, Aix Marseille Université, Marseille, France;* [2]*Department of Psychology, New York University, New York, New York; and* [3]*Center for Neural Science, New York University, New York, New York*

Submitted 14 June 2018; accepted in final form 8 September 2018

Guillaume A, Fuller JR, Srimal R, Curtis CE. Cortico-cerebellar network involved in saccade adaptation. *J Neurophysiol* 120: 2583–2594, 2018. First published September 12, 2018; doi:10.1152/jn.00392.2018.—Saccade adaptation is the learning process that ensures that vision and saccades remain calibrated. The central nervous system network involved in these adaptive processes remains unclear because of difficulties in isolating the learning process from the correlated visual and motor processes. Here we imaged the human brain during a novel saccade adaptation paradigm that allowed us to isolate neural signals involved in learning independent of the changes in the amplitude of corrective saccades usually correlated with adaptation. We show that the changes in activation in the ipsiversive cerebellar vermis that track adaptation are not driven by the changes in corrective saccades and thus provide critical supporting evidence for previous findings. Similarly, we find that activation in the dorsomedial wall of the contraversive precuneus mirrors the pattern found in the cerebellum. Finally, we identify dorsolateral and dorsomedial cortical areas in the frontal and parietal lobes that encode the retinal errors following inaccurate saccades used to drive recalibration. Together, these data identify a distributed network of cerebellar and cortical areas and their specific roles in oculomotor learning.

NEW & NOTEWORTHY The central nervous system constantly learns from errors and adapts to keep visual targets and saccades in registration. We imaged the human brain while the gain of saccades adapted to a visual target that was displaced while the eye was in motion, inducing retinal error. Activity in the cerebellum and precuneus tracked learning, whereas parts of the dorsolateral and dorsomedial frontal and parietal cortex encoded the retinal error used to drive learning.

cerebellum; motor learning; oculomotor vermis; precuneus; saccade adaptation

INTRODUCTION

To keep the sensory and motor systems in registration, the brain tracks and uses errors to inform and drive changes in the transformation of visual signals into motor commands (for review see Krakauer and Mazzoni 2011; Shadmehr et al. 2010; Wolpert and Flanagan 2016). In the case of saccades, the fast eye movements that reorient gaze, this process is referred to as saccade adaptation (for review see Hopp and Fuchs 2004; Pélisson et al. 2010). Although the muscles that control the eyes are perturbed over time because of a myriad of factors (e.g., development and aging, disease processes, and even fatigue during the course of a day), our saccades remain largely accurate because of these adaptive processes. The mechanisms that control saccade adaptation appear to be in continuous operation, using the accuracy of each and every saccade as an input (Srimal et al. 2008).

In the laboratory, the way one traditionally studies saccade adaptation involves displacing a visual target that is the goal of a saccade while the saccade is in flight (McLaughlin 1967). Transaccadic blindness causes the oculomotor system to interpret the retinal error as motor command error. Over many trials, the landing position of the saccade adapts; the end point gradually shifts toward the displaced target and away from the initial visual target. Neurophysiological studies in animals (e.g., Barash et al. 1999; Optican and Robinson 1980) and neuropsychological studies of humans with lesions (e.g., Panouillères et al. 2013; Waespe and Baumgartner 1992) have provided clear evidence that the cerebellum, especially the oculomotor vermis (lobules VI and VII of the vermis), is critical for saccade adaptation (Herman et al. 2013; Hopp and Fuchs 2004; Pélisson et al. 2010; Prsa and Thier 2011).

Previous neuroimaging studies using positron emission tomography (PET) and functional magnetic resonance imaging (fMRI) have investigated whether activity changes in the human cerebellum correlate with saccade adaptation (Blurton et al. 2012; Desmurget et al. 1998, 2000; Gerardin et al. 2012). Unfortunately, the results from these studies have been inconsistent. The PET studies of Desmurget et al. (1998, 2000) found that blood flow changes in the oculomotor vermis occurred during saccade adaptation. The fMRI study by Blurton et al. (2012) failed to replicate this effect. Using multivoxel pattern analysis, Gerardin et al. (2012) reported that the pattern of activity within the lateral cerebellum (lobules VIIb–VIIIa) was distinct during saccade adaptation, but the classification analysis was not performed in the oculomotor vermis. Results across these studies were inconsistent in cortical areas as well.

There are a number of potential reasons for the inconsistency of past imaging studies of saccade adaptation, which we aimed to address here. First, the previous studies all used a region of interest (ROI) approach, focused on different ROIs, and even used different criteria to define ROIs. Obviously, this makes it difficult to make direct comparisons across experiments in attempts to replicate and establish consistency. Second, computational theories of motor control postulate the existence of inverse and forward models to produce the motor commands and predict their effects (Haith and Krakauer 2013; Shadmehr et al. 2010; Shadmehr and Krakauer 2008; Tin and Poon 2005).

Address for reprint requests and other correspondence: C. E. Curtis, New York Univ., 6 Washington Pl., 8th Fl., New York, NY 10012 (e-mail: clayton.curtis@nyu.edu).

According to these theories, sensory prediction errors (i.e., differences between the predicted error and the actual error for a given movement) drive motor learning (Shadmehr et al. 2010; Wolpert et al. 2011; Wong and Shelhamer 2011). Hence, during adaptation several subprocesses are simultaneously in play, including actual error registration, predicted error estimation, and, by comparing these two signals, the computed sensory prediction error. Each of these subprocesses is used to optimize learning through the updating of internal models, including both inverse and forward models (Aprasoff and Donchin 2012; Chen-Harris et al. 2008). Perhaps the inconsistency in previous neuroimaging studies of saccade adaptation is due to their measurements being more or less sensitive to different subprocesses of adaptation. Third, uncontrolled factors correlated with saccade adaptation might confound clean measurements related to learning. Most notably, the changing amplitudes of corrective saccades are highly correlated with learning and could be driving much of the signal measured by PET and fMRI. The hallmark of saccade adaptation is that saccade landing gradually shifts toward the displaced target over dozens of trials. However, after inaccurate saccades people make corrective saccades to the displaced target. During adaptation, these corrective saccades get smaller at the same rate that the initial saccades are adapting. Therefore, what previous studies may be measuring during adaptation is changes in corrective saccade amplitude and not processes directly related to learning (for similar arguments see Schlerf et al. 2012; Seidler et al. 2002). Indeed, the amplitudes of microsaccades, even when they are $<1°$, predict the amplitudes of fMRI signal (Tse et al. 2010), demonstrating that the effects of even small saccades need to be controlled.

Here we addressed these three limitations by making measurements from the whole brain during saccade adaptation, modeling neural responses predicted by theoretical subcomponent processes involved in motor learning (e.g., error measurement and adaptive gain modification), and using a modified adaptation procedure that avoids the potential confounding influence of changing corrective saccade amplitudes. With regard to the last point, we used a clamping procedure in which we displaced the visual saccade target during the saccade but only for a short time, after which we placed the target near the measured point of gaze. The goal was to break the correlation between corrective saccade amplitude and learning by affecting the number and amplitude of corrective saccades. Critically, previous behavioral studies that have used this procedure still found that saccades adapt (Havermann and Lappe 2010; Noto and Robinson 2001; Wallman and Fuchs 1998), indicating that corrective saccades, per se, do not drive learning. Finally, the mechanisms that control sensorimotor adaptation may differ between externally triggered, reactive saccades and internally triggered, voluntary saccades (Alahyane et al. 2007, 2008; Cotti et al. 2007, 2009; Gerardin et al. 2012). Even the direction of adaptation, a shift backward resulting in a decrease in saccade gain vs. a shift forward resulting in an increase in gain, may require distinct mechanisms (see for review Hopp and Fuchs 2004; Pélisson et al. 2010). In brief, these procedures allow us to now describe a cerebral and cerebellar network whose activity tracks different subcomponent processes involved in the more traditionally studied reactive saccade adaptation.

MATERIALS AND METHODS

Participants

Twelve neurologically healthy participants (right-handed; 24–40 yr old; 5 women, 7 men) participated in the study after giving written informed consent. All had normal or corrected to normal visual acuity. All procedures were reviewed by the human subjects Institutional Review Board at New York University and were carried out in accordance with the approved guidelines.

Experimental Procedures

Participants, lying in the supine position within the fMRI scanner, viewed off a mirror stimuli projected onto a screen within the bore. Movements of the left eye were recorded with an EyeLink 1000 system (SR Research) with a sampling rate of 1,000 Hz. A short training phase allowed participants to be familiarized with visual stimuli and the task. Each participant performed one scanning session of 250 trials, divided into three phases. Participants were not told that there were phases and were not aware that there would be intrasaccadic displacements of the visual targets. They were simply told that we were interested in how the brain produces visually guided saccades and were asked to produce accurate but fast saccades to acquire peripheral targets. In *phase 1* (Preadapt; 50 trials), we established baseline saccade accuracy by measuring saccades while participants simply made visually guided saccades to visual targets (black dots on a gray background). Participants fixated a white cross at 5°, 6°, 7°, 8°, or 9° to the right of a screen's center for 2 s. After 0–200 ms (50-ms steps), the fixation cross disappeared and a black target appeared 16° to the left. Participants made leftward saccades to acquire this target. In *phase 2* (Adapt; 150 trials), we induced retinal error by displacing the visual target intrasaccadically (i.e., during the flight of the saccade) with the goal of measuring how saccades adapted to this perturbation. When the leftward saccade was initiated and detected through a velocity threshold of 30°/s, the target was displaced by 3° to the right. Therefore, even when a perfectly accurate saccade was generated, it resulted in retinal error. However, we modified the standard procedure (McLaughlin 1967). After 160 ms during which the participant could perceive the retinal error induced by the backstep, we then displaced the visual target to 0.5° to the left of fixation. In the present study, saccades to the target 16° to the left mostly lasted between 55 and 65 ms. The velocity threshold for target displacement was crossed ~25–30 ms after saccade onset. Therefore, the target was visible on the retina for an average of 134.6 (±11.3) ms before displacement. Preliminary studies indicated that the timing and position of the target displacement reduced the frequency and amplitude of corrective saccades. The target remained on for 2 s, after which the fixation cross for the next trial reappeared. Fixation time was randomized across trials to aid decomposition of the fMRI signal variance related to learning and saccade generation and to reduce anticipatory saccades. See Fig. 1*A* for a depiction of the classic and modified versions of the task. In *phase 3* (Deadapt; 50 trials), trials were the same as during the baseline phase and allowed us to observe the deadaptation process.

Image Acquisition

MRI data were collected with a 3.0-T head-only scanner (Allegra, Siemens) at the Center for Brain Imaging at New York University. Images were acquired with a custom four-channel phased-array receive coil (NOVA Medical) placed over lateral frontal and parietal cortices. For the functional data, we used a T2*-sensitive echo planar imaging pulse sequence. Scanning parameters were repetition time (TR), 2,000 ms; echo time, 30 ms; flip angle, 75°; 36 slices; 3 × 3 × 4 mm voxels. At the end of each scanning session, T1-weighted low-resolution anatomical images were first collected with the same slice prescriptions as the functional data. Finally, high-resolution (1 ×

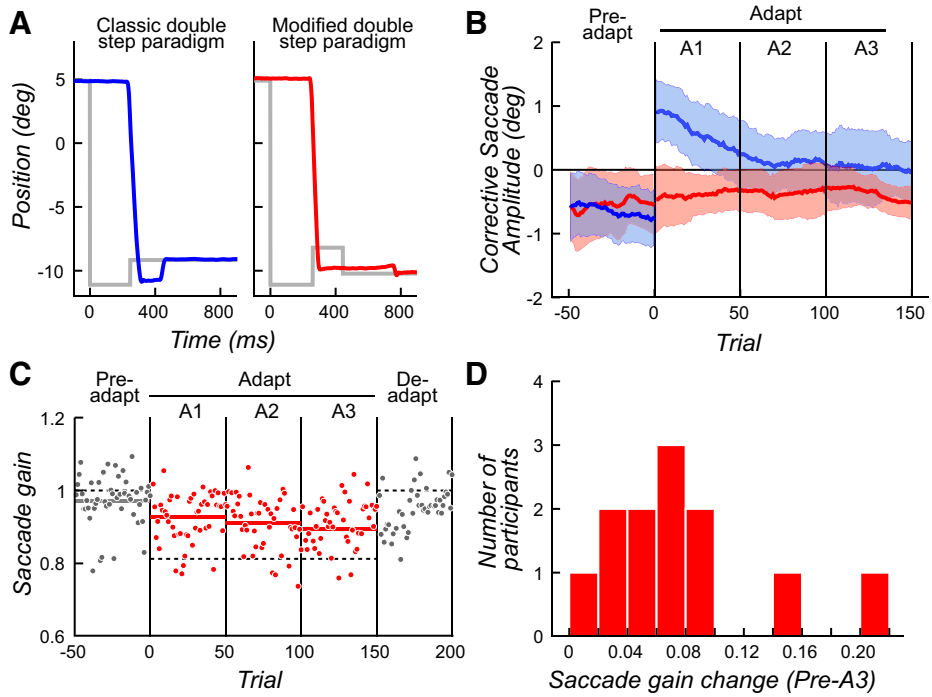

Fig. 1. Modified backstep paradigm used in the present study and behavioral results. *A*: examples of typical horizontal eye position traces for trials early in the adaptation phase. Gray lines represent target position. *Left* (blue): the classic backstep paradigm with a backward target step during the saccade, which induces a backward corrective saccade (data from Srimal et al. 2008). *Right* (red): in our modified paradigm, the backstepped target was presented for only 160 ms and then was placed 0.5° to the left of fixation. *B*: amplitude of corrective saccades as a function of the trial number across all participants. Mean amplitude was calculated with a sliding window of 10 trials. Shaded areas correspond to ±1 SD. Blue curve corresponds to values obtained with the classic backstep paradigm (data from Srimal et al. 2008) and red curve to values obtained with our modified backstep paradigm. Note how the amplitudes of corrective saccades track learning only in the classic version. *C*: saccade gain as a function of trial number for a representative participant. An experimental session was divided into 5 phases of 50 trials each: Preadapt, Adapt (A1, A2, A3), and Deadapt. Thin dashed horizontal lines demark the amplitude of the target. Thick solid horizontal lines correspond to mean saccade gain for each phase. Note how saccade gain decreases in each Adapt phase and then rebounds in the Deadapt phase. *D*: distribution of saccade gain changes from Preadapt to A3 phases for each participant.

1 × 1 mm) T1-weighted scans were acquired for registration, segmentation, and display.

Data Preprocessing

Functional imaging data were preprocessed and analyzed with AFNI (https://afni.nimh.nih.gov/; Cox 1996). The preprocessing of the functional data contained the following steps. Every image was upsampled to 2 × 2 × 2 mm. The first two volumes of each run were discarded to allow for T1 equilibration effects. Images were then slice-time corrected and were aligned with the first TR of the first run. All images were smoothed with a Gaussian kernel (full width at half maximum = 4.0 mm), and finally the fMRI signal was scaled to 100. The anatomical scan was also aligned with the volume of the first TR of the first functional run to allow activity localization. After this alignment, it was normalized to the Montreal Neurological Institute (MNI) space (template N27caez in AFNI) to allow the normalization of functional statistical results with the command @auto_tlrc of AFNI.

fMRI Design and Statistical Analyses

Each participant performed 10 runs, 25 trials each, that each lasted 284 s (142 TRs). The duration of a trial was pseudorandomly chosen from a gamma distribution ranging from 4 to 14 TRs, where 70% of all trials had a duration of 5–8 TRs. The visual target occurred at the beginning of the first TR plus 0–200 ms (50-ms step) to introduce some temporal uncertainty. The first two runs were always baseline Preadapt trials, followed by six runs of Adapt trials and finished with the last two runs of the Deadapt trials.

After the preprocessing, images were analyzed in native space for each participant by the general linear model (GLM) approach with the 3dDeconvolve function of AFNI. This function allows creation of polynomial regressors (3rd-order polynomial, 4 regressors) separately for each run to account for baseline level and slow drift of signal. Six regressors were also created to account for potential activity variation related to head movements. To search for activity variations related to the task we ran four separate GLMs. In the first, we used a regressor with delta functions time-locked to saccade initiation and convolved with the default hemodynamic function in AFNI (GAM). This regressor modeled each visually guided saccade across all five phases of the experiment. β values for this regressor allowed evaluation of transient blood oxygen level-dependent (BOLD) variation related to saccades. The second GLM modeled the first four trial phases (Preadapt, A1, A2, and A3). We split the Adapt phase into three blocks, A1, A2, and A3, so we could estimate several combinations of BOLD variation during the experiment (e.g., Preadapt vs. A1 to measure changes at the beginning of the adapt phase). We also ran follow-up GLMs that allowed us to conduct parametric analyses of learning-related changes during the three Adapt phases. As in the first GLM, we modeled each saccade with a delta function. To estimate BOLD changes associated with a decrease in saccade gain during adaptation, we scaled the height of each delta function of a second regressor by the gain change of that saccade (*trial n*) relative to the previous saccade (*trial n − 1*). Values for this regressor were demeaned for orthogonalization and convolved with a hemodynamic response function. Only saccades showing a gain decrease were modeled, in order to target adaptation specifically. To control for changes associated with random fluctuations in saccade amplitude, we ran a parametric analysis aimed at estimating BOLD changes associated with the reduction in amplitude

of saccades during the Preadapt phase, in the absence of adaptation. To make the control analysis as similar as possible, we only modeled saccades showing a gain decrease from the previous trial. Finally, we ran another parametric analysis aimed at estimating BOLD changes associated with the amount of retinal error following each saccade during the three Adapt phases. Here, the height of each delta function of a second regressor time-locked to the saccades was scaled by distance between the backstepped target and the saccade end point. Because hypermetric errors drive learning, we only modeled saccades with hypermetria.

For each GLM, group analyses were conducted separately for the cerebrum and the cerebellum. For the cerebrum, maps of β values of interest, or of difference in β values, in native space were normalized to MNI space with the transformation obtained through the normalization of the anatomical scan (see above). For the cerebellum, to improve the normalization procedure required for the group analysis we used the SUIT toolbox [spatially unbiased infratentorial template (Diedrichsen 2006)]. The cerebellum of each participant was isolated and normalized to the SUIT atlas. The resulting transformation was used to bring results of first-level analyses (the 4th GLM described above) into SUIT space, thus improving alignment (see Diedrichsen 2006).

Group-level analyses consisted of one-way ANOVAs (with phases as levels) and *t*-tests on the β values or differences in β values. For each group analysis, the level of significance was set initially to P uncorrected < 0.005 at a voxel level that corresponded to $t = 3.580$. To account for multiple comparisons, we used results of Monte Carlo simulations (AFNI 3dClustSim program) giving the minimum size of a cluster a threshold of P corrected < 0.05. Results were 250 voxels for the cerebrum and 150 voxels for the cerebellum, considered separately because isolated with the SUIT toolbox. The only analysis for which chosen values were different was that to globally identify saccade areas in which activations were large and robust. We used a P uncorrected < 0.002 ($t = 4.033$) and a minimum cluster size of 1,000 voxels. For visualization purposes, the surviving clusters were projected on the cortical surfaces for the Colin 27 brain and on a flat representation of the cerebellar cortex (SUIT toolbox).

RESULTS

Behavior

We used a modified backstep paradigm with the aim of inducing saccade adaptation while removing the correlation of corrective saccade amplitude and the process of adaptation. Figure 1*A* depicts example trials obtained with this modified protocol (Fig. 1*A*, *right*) compared with a trial obtained with the classic backstep paradigm (Fig. 1*A*, *left*; data from Srimal et al. 2008). It should be noted that the corrective saccade was minimized by displacing the backstepped target near the point of gaze. Compared with the Preadapt phase, the frequency of corrective saccades did not change during the Adapt phase [$t(11) = -1.71$, $P = 0.12$]. Critically, the amplitude of corrective saccades was effectively constant across the phases and thus did not predict learning. Compared with the Preadapt phase, the amplitudes of corrective saccades did not change during the Adapt phase [$t(11) = -0.70$, $P = 0.49$]. In Fig. 1*B*, we plot the amplitudes of corrective saccades across trials in the Preadapt and Adapt phases. During the Preadapt phase, small leftward corrective saccades compensate for slightly hypometric initial saccades, as expected. During the Adapt phase, small rightward corrective saccades compensate for overshooting the backstepped target in the classic paradigm, and the decreasing amplitudes of these corrective saccades track saccade adaptation closely (Fig. 1*B*). However, in our modified double-step paradigm the rapid placement of the visual target near the fovea resulted in small leftward corrective saccades that were of the same amplitude across the Preadapt and Adapt phases (Fig. 1*B*). Although the amplitudes of corrective saccades did not change during the phases of the task, participants still showed strong evidence of saccade adaptation similar to previous behavioral studies (Noto and Robinson 2001; Wallman and Fuchs 1998). In Fig. 1*C*, we plot the change in saccade gain over the trials in each phase of the task for a representative participant. Note how the gain of saccades is just slightly hypometric during the Preadapt phase and then becomes more and more hypometric during the Adapt phases. Moreover, one can observe the slow return of the original gain during the Deadapt phase, when the target no longer backsteps. In Fig. 1*D*, we show the distribution of saccade gain changes during adaptation for each participant. We computed the gain difference between the Preadapt phase and the third period of the Adapt phase (A3) for each participant. A paired *t*-test comparing mean gain in Preadapt vs. A3 demonstrated a statistically significant decrease in saccade gain [$t(11) = 4.83$, $P = 0.0005$) representing 39% of what would be a complete adaptation. At the single-participant level, 10 of the 12 participants showed a significant reduction in gain. Overall, these behavioral results enable us to now examine how BOLD signal changes in the human brain might predict processes associated with saccade adaptation without the confounding influence of corrective saccades.

Imaging Results

Saccade generation. Before analyzing BOLD changes related to saccade adaptation, we first identified areas active during the production of visually guided saccades without regard to the experimental phase. This analysis verified the sensitivity of our measurements and identified the classic saccade network (Curtis and Connolly 2008; Grosbras et al. 2005; Lynch and Tian 2006) (Fig. 2). Particularly strong responses were noted in dorsolateral frontal and parietal cortex, including the precentral and intraparietal sulcus. Along the medial wall, we observed responses in the paracentral sulcus, the dorsal anterior cingulate, and the precuneus. Classic visual areas in occipital cortex were also active, because of the visual saccade targets and other visual inputs sweeping across the retina with saccades to the target and back to fixation. Saccades drove activity in the cerebellum, too. This included the oculomotor vermis, in lobules VI and VII, and the lateral cerebellum, in lobules VI and VIIb/VIIa. Recall that our task involved making 16° leftward saccades on each trial. Not surprisingly, we found that generating visually guided leftward saccades caused slightly larger BOLD activity in the right cortex and the left cerebellum. This aligns with the contraversive control of saccades in cortex and the ipsiversive control of saccades in the cerebellum. Moreover, we find this although participants always made rightward saccades to acquire fixation and begin the next trial.

Adaptive processes. Our next goal was to identify brain areas whose activity changed during the course of adaptation. We conducted a group-level repeated-measures ANOVA on the β estimates for each phase (4 phase levels: Preadapt, A1, A2, A3), which resulted in no cluster surviving the threshold for multiple comparisons (see MATERIALS AND METHODS). A closer examination of the data suggested a couple of reasons

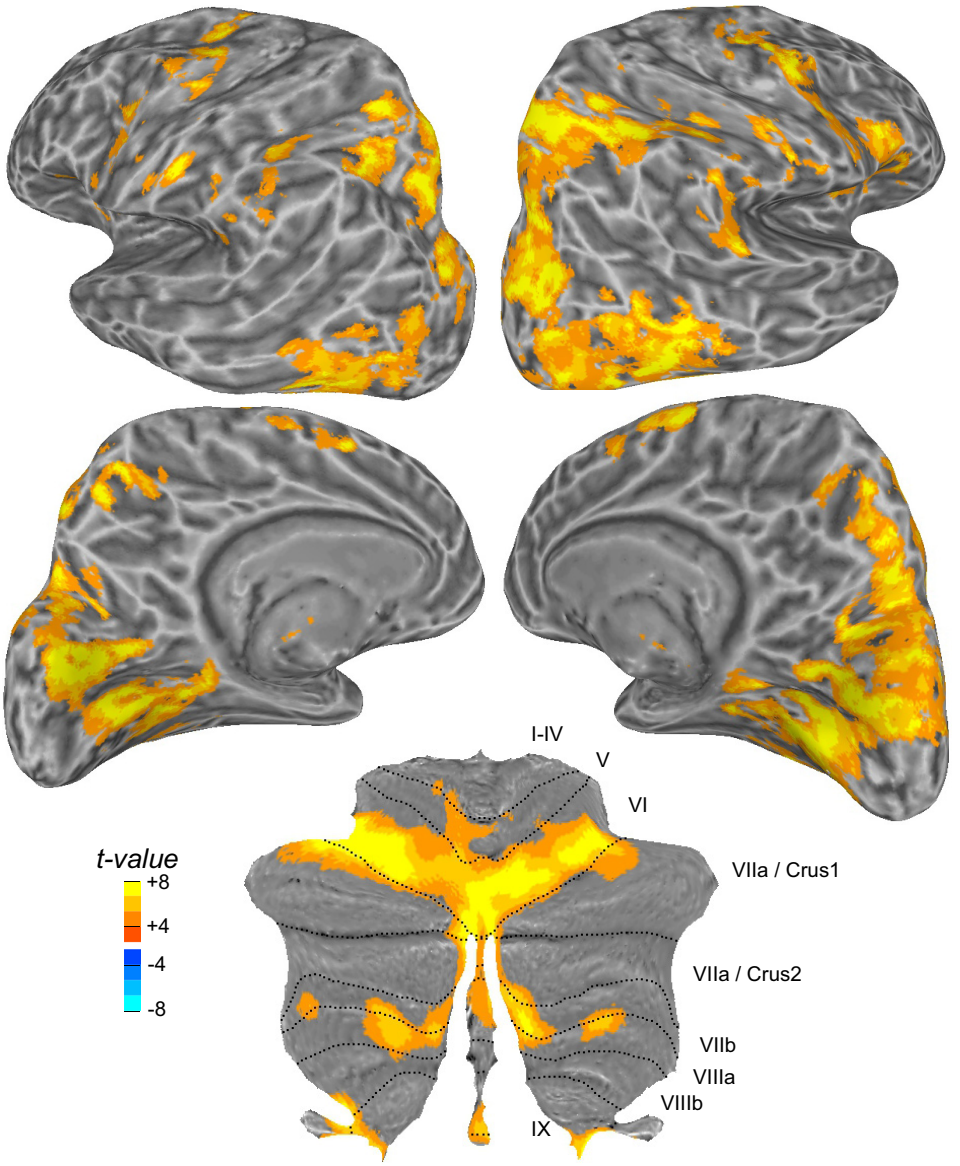

Fig. 2. Cortical and cerebellar activity during visually guided saccades. *t*-Statistic maps are projected onto an inflated model of the left and right hemispheres of the human brain (lateral and medial views), where dark gray corresponds to the sulcal folds and light gray to the gyral convexities. For the cerebellum, the results are projected on a flat representation of the cerebellum. Roman numerals denote cerebellar lobules according to the Larsell notation (Schmahmann et al. 2000). Note the larger activations in the right cortex and in the left cerebellum during leftward saccades.

for this null result. First, several participants showed quite strong changes across the phases, and these participants were the ones who showed the strongest behavioral evidence of saccade adaptation. Second, the bulk of the learning, based on rate of change of the saccade gain, was most limited to the first phase of the adapt period (A1). Thus we conducted another ANOVA, limiting the analysis to the Preadapt and A1 phases and using each participant's level of saccade adaptation as a covariate (Fig. 3*A*). In fact, Desmurget et al. (1998, 2000) used this exact same procedure to identify cerebellar activity during learning. We simply computed the saccade gain change between the Preadapt and A1 phases for each participant and used this as a covariate in the analysis testing for differences in BOLD activity between Preadapt and A1 phases. In Fig. 3*B*, we plot the distribution of gain changes that were used as the covariate. Now, when taking into account the adaptation level of each participant, we found three statistically significant clusters (Fig. 3*A*, Table 1). In the left oculomotor vermis (Crus I and II regions of lobule VIIa) and the right precuneus, we found that increases in BOLD activity in the A1 phase compared with the Preadapt phase were larger in participants whose saccades adapted the most. We also found one area, an intermediate region of the right cerebellum (Crus II), whose BOLD activity decreased in A1 compared with Preadapt, again as a function of the level with which participants' saccades adapted. Curious about the two participants whose saccade gain increased between the Preadapt and A1 phases (Fig. 3*B*), we plotted for each of these three clusters the difference between the β values in these two phases against each participant's saccade gain change (Fig. 3*C*). Here, one can clearly see the linear relationship between changes in BOLD activity and changes in saccade gain during learning. Interestingly, the two participants who showed gain increases showed BOLD decreases in the right precuneus and left oculomotor vermis.

Next, we expanded our search for learning-related signals across the all three Adapt blocks. The efficacy of the mechanisms that support learning likely varies randomly across trials. Indeed, behaviorally one can see variability in the reduction of saccade gain during the course of adaptation (Fig. 1*C*). We reasoned that trials in which the saccade gain decreased rela-

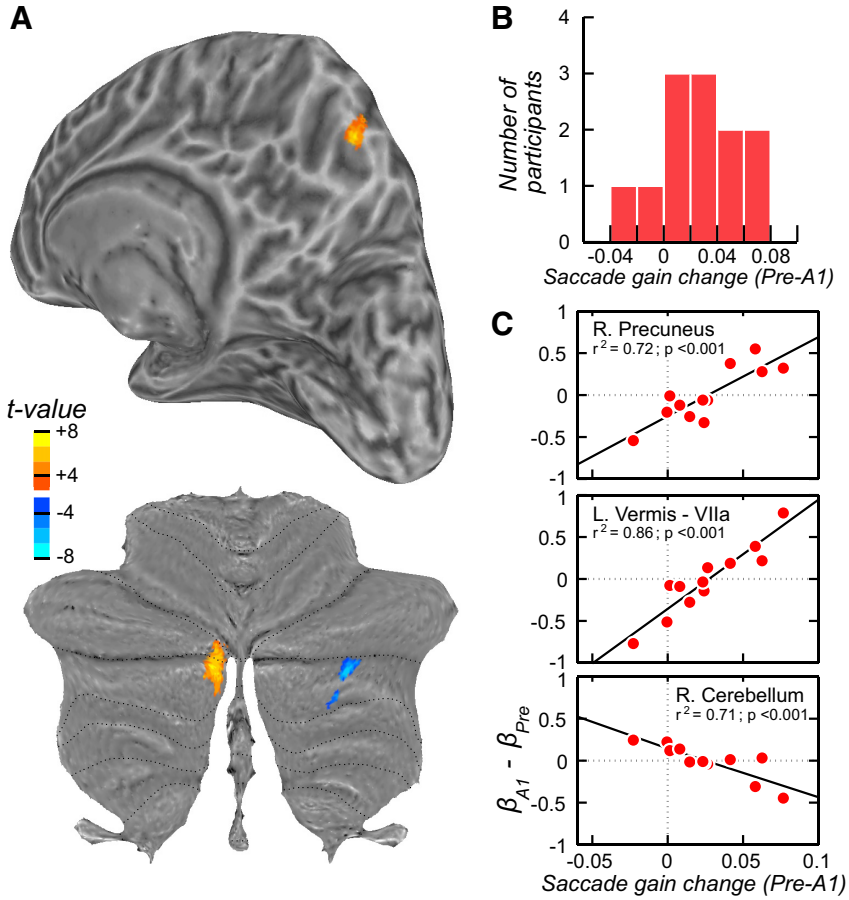

Fig. 3. Cortical and cerebellar activations related to adaptation of saccades. *A*: results of the group analysis for the contrast between the Preadapt and A1 (Adapt) phases. During the first phase of Adapt when the saccade gain decreased the most, blood oxygen level-dependent (BOLD) signal increased in the oculomotor vermis (lobule VIIa) and on the medial wall of the parietal cortex, in the right precuneus. There was also a decrease in activity in the right cerebellar hemisphere (lobule VIIb/Crus 2). *B*: mean gain change between these 2 phases for each participant, which was entered as a covariate in the general linear model (see MATERIALS AND METHODS). *C*: for each cluster in *A*, we graph the covariation between the change in BOLD signal (β) during saccade adaptation and the degree of saccade gain change during adaptation.

tive to the previous trial were trials in which the mechanisms that drive learning were most robust, and more likely to be measurable. Therefore, we identified these trials in each participant and calculated the gain difference between *trial n* and *trial n − 1* for all trials in the Adapt phase (A1, A2, and A3). We then ran a GLM analysis, again focused on trials when the saccade gain decreased, that used the size of this gain difference as a parametric regressor; each saccade was modeled by

Table 1. *Location and size of significant clusters of activations in each of the GLMs*

	Hemisphere	MNI Coordinates of Maximum, mm			Cluster Size, voxels	*P* (cluster)
		X	*Y*	*Z*		
GLM phase A1 vs. Preadapt, with gain change as a covariate						
Cerebellar vermis lobule VIIa (Crus 1 and 2)	L	−7	−79	−30	903	<0.001
Cerebellar hemisphere (Crus 2)	R	25	−62	−42	552	<0.001
Precuneus	R	4	−65	51	261	<0.03
GLM parametric regressor: gain change from trial n − 1 to trial n						
Supramarginal gyrus	R	53	−35	49	347	<0.005
Precuneus	R	11	−69	46	334	<0.005
GLM parametric regressor: error (hypermetria)						
Calcarine gyrus	L	−10	−60	−1	11,091	<0.001
Calcarine gyrus	R	21	−62	10	8,063	<0.001
Superior occipital gyrus (V3A)	R	19	−80	25	4,132	<0.001
Superior occipital gyrus (V3A)	L	−24	−78	24	3,127	<0.001
Parieto-occipital sulcus	L	−13	−73	21	1,235	<0.001
Parieto-occipital sulcus	R	20	−60	27	1,025	<0.001
Cerebellar hemisphere lobule VI	R	23	−71	−21	791	<0.001
Cerebellar hemisphere lobule V	L	−6	−61	−7	736	<0.001
Intraparietal sulcus	L	−27	−58	47	730	<0.001
Precentral sulcus	R	40	−7	54	652	<0.001
Anterior insula	R	57	11	−2	576	<0.001
Temporo-parietal junction	R	60	−41	25	486	<0.005
Medial superior frontal gyrus	R	6	−1	58	255	<0.03

GLM, general linear model; L, left; MNI, Montreal Neurological Institute; R, right.

a delta function whose height was scaled by the demeaned difference in saccade gain. This analysis produced two significant clusters after correction for multiple comparisons. The same region of the right precuneus identified by the previous analysis was again observed, providing further evidence for its role in the saccade adaptive process (Fig. 4*A*). Although the exact coordinates slightly differed (Table 1), lowering the threshold ($P = 0.01$ rather than $P = 0.005$) resulted in a complete overlap of the two clusters (not shown). On the lateral parietal cortex, increases in activity in the right supramarginal gyrus also predicted significant trial-to-trial gain changes (Fig. 4*B*). We wanted to rule out that these results could be driven by trial-by-trial gain decreases in saccade amplitude unrelated to changes due to adaptation. Thus we performed a control analysis using the data from the Preadapt phase. Indeed, the mean change in saccade gain between two consecutive trials showing a gain decrease during the Preadapt phase trended toward being smaller compared with the Adapt phases [1.03° vs. 1.27°; $t(11) = 1.99$, $P = 0.07$]. Therefore, using data from the Preadapt phase, we ran another parametric GLM analysis in which we modeled each saccade as a delta function whose height was scaled by the demeaned difference in saccade gain. No voxels were significant, suggesting that our findings with regard to the precuneus and supramarginal gyrus were not due to random changes in saccade amplitude but instead were due to learning.

Saccade targeting errors. Adaptive processes are initiated when motor errors are detected. Next, we aimed to identify areas in the brain whose activity is involved in the detection and/or processing of these motor errors. We used the amplitude of saccade error induced by the backstepped target as our measure of motor error. This metric is also the degree of retinal error between the visual target and the saccade landing position. We ran a GLM analysis that used the size of saccade error as a parametric regressor; each saccade was modeled by a delta function whose height was scaled by the demeaned saccade error. The goal of learning was to reduce hypermetria induced by the backstepped target, and saccade hypermetria and hypometria are represented differently in the brain (Liem et al. 2013; Pélisson et al. 2010). Therefore, we focused on the hypermetric saccade errors that may be driving learning. We find that the size of saccade error evoked large bilateral activations in visual areas (calcarine sulcus), in the parieto-occipital sulcus, and in the superior occipital gyrus (Fig. 5). Saccade error also drove activation in the left hemisphere of the intraparietal sulcus and the right hemisphere of the superior precentral sulcus, the paracentral sulcus, and the temporo-parietal junction. Consistent with Blurton et al. (2012), we observed activity in the insula, but only in the right hemisphere. Finally, two clusters in the cerebellum were sensitive to the amplitude of saccade errors, including the left cerebellum (lobule V) and the right cerebellum (lobule VI), both of which were identified by general saccade generation (Fig. 2).

DISCUSSION

Using fMRI and concurrent eye tracking, we aimed to identify a network of human cerebral and cerebellar brain areas involved in saccade adaptation. Moreover, by using a modified version of the classic backstep paradigm and modeling fMRI responses conditioned on parametric measures associated with learning, we both avoided confounds and isolated subprocesses of saccade adaptation. In summary, we observed clear behavioral evidence of saccade adaptation even when the duration of retinal error was so short that corrective saccade amplitude did not track learning. This was critical because it allowed us to then isolate signals related to learning and not corrective saccades. We found that activity in the oculomotor vermis increased during saccade adaptation in a manner that was proportional to the strength of adaptation within the learner. We found a similar pattern in a cortical area on the medial wall of the parietal cortex, in the precuneus. A follow-up analysis showed that activity in the precuneus also tracked the trial-to-trial reductions in saccade gain during adaptation, further supporting its role in saccade learning. Distinct from these learning effects, we found that portions of the dorsolateral and dorsomedial frontal and occipital cortex responded in a monotonically increasing manner as the postsaccade retinal error grew. Below, we interpret these findings in the context of previous theoretical and empirical work.

Lesions to the monkey (Barash et al. 1999; Optican and Robinson 1980; Robinson et al. 2002; Takagi et al. 2003) and human cerebellum, more specifically the dorsal part of the vermis known as the oculomotor vermis (Alahyane et al. 2008; Straube et al. 2001; Tseng et al. 2007; Waespe and Baumgartner 1992), impair oculomotor learning. Transcranial magnetic stimulation of the human oculomotor vermis impairs saccade adaptation (Jenkinson and Miall 2010; Panouillères et al.

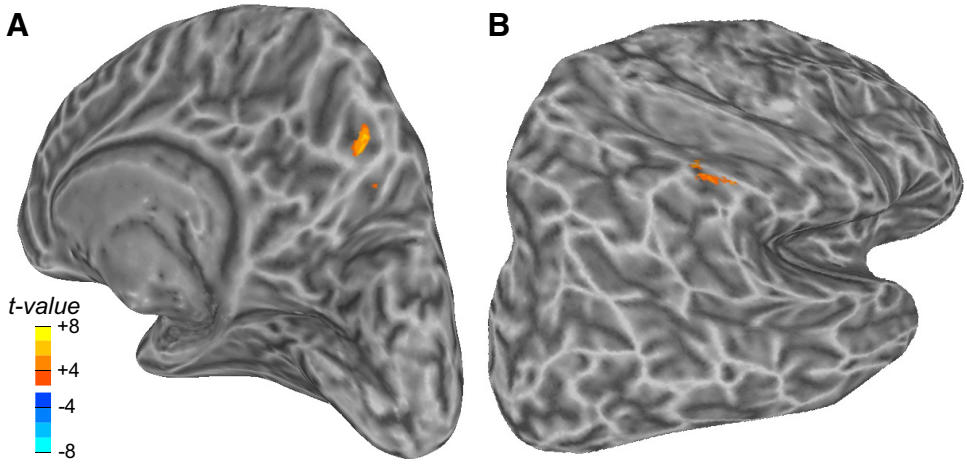

Fig. 4. Activity in contraversive precuneus (*A*) and supramarginal gyrus (*B*) track reductions in gain during saccade adaptation.

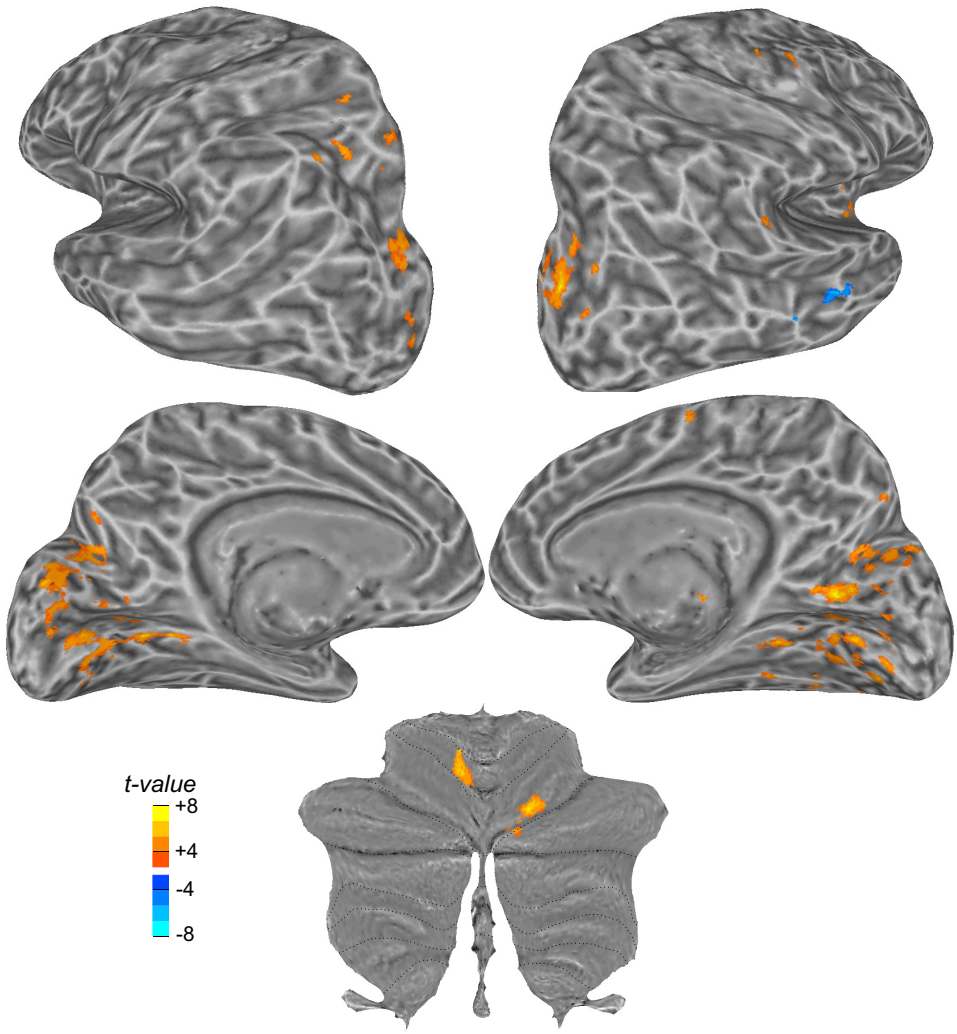

Fig. 5. Cortical and cerebellar activations obtained in the parametric analysis based on the size of saccade error introduced by the target step. Blood oxygen level-dependent (BOLD) variations with amplitude correlated to the size of the error were found bilaterally in the calcarine sulcus, in the parieto-occipital sulcus, and on the superior occipital gyrus. One cluster was found in the intraparietal sulcus of the left hemisphere and 2 others in the frontal cortex of the right hemisphere: 1 in the precentral sulcus and 1 on the medial superior frontal gyrus. Activations were also observed in the right anterior insula and in the right temporo-parietal junction. Two clusters were found in the cerebellum (left lobule V and right lobule VI).

2012). Using PET, Desmurget et al. (1998, 2000) demonstrated that blood flow in the oculomotor vermis bilaterally increased during saccade adaptation and this increase depended on the degree to which individuals adapted. We replicate and extend their results here. We found that BOLD signal increased during adaptation proportional to the strength of adaptation within each learner and did so selectively in the ipsiversive oculomotor vermis. The higher spatial resolution of fMRI over PET and our improved registration of cerebellums both may have allowed us to measure the lateralized effect. Indeed, electric microstimulation of the macaque oculomotor vermis evokes ipsiversively directed saccades with very short latencies (~15 ms) (Fujikado and Noda 1987). Purkinje cells in the oculomotor vermis send inhibitory efferents through the caudal fastigial nucleus that influence the metrics, including the amplitude, of saccades via their direct effects on the brain stem (Yamada and Noda 1987). For example, this inhibitory circuit could dampen the amplitude of saccades by reducing their duration. Consistent with our results, unilateral injection of muscimol to caudal fastigial nucleus in monkeys causes hypermetric ipsiversive saccades (Robinson et al. 2002), and one would predict that during learning where saccades are adapting toward hypometria, the ipsilateral cerebellum would be most important. The fMRI study of saccade adaptation by Blurton et al. (2012) did not find learning-related effects in the oculomotor vermis, perhaps because they did not use learning performance as a covariate.

Interestingly, our findings suggest that the dorsal precuneus may be a key cortical area in oculomotor learning. We found that BOLD signal in the contraversive precuneus increased during adaptation proportional to the strength of adaptation. Moreover, activity in the precuneus predicted trial-to-trial reductions in saccade gain during adaptation. To the best of our knowledge, this is the first time that the precuneus has been linked to reactive saccade adaptation. Previous imaging studies did not include it in the list of a priori ROIs (e.g., Blurton et al. 2012; Desmurget et al. 1998, 2000), although the dorsal precuneus is considered to be a part of the saccade network (Cavanna and Trimble 2006; Margulies et al. 2009) and saccade production reliably evokes activity in the human precuneus (e.g., Berman et al. 1999; Grosbras et al. 2005; Lynch and Tian 2006; Müri 2006). We too find strong responses in the dorsal precuneus during saccade generation regardless of learning (Fig. 2). Interestingly, the adaptation of voluntary, but not reactive, saccades activates a nearby area (Gerardin et al. 2012), in contrast to the present results, suggesting that future work needs to address to what degree different mechanisms are involved or if these differences are the result of different experimental methods. This cortical area in humans may correspond to a medial parietal (MP, PGm, or 7m) area in

macaques (Cavanna and Trimble 2006; Kravitz et al. 2011; Leichnetz 2001; Pandya and Seltzer 1982; Thier and Andersen 1998). MP is interconnected with the oculomotor network, including the frontal eye field, lateral intraparietal area, and the intermediate layer of the superior colliculus (SC) (Leichnetz 2001). Intriguingly, microstimulation of neurons in the MP evokes saccades, but the amplitude of these evoked saccades depends on the starting orbital position of the eye (Thier and Andersen 1998). A gaze shift to acquire a target in retinal space is naturally composed of both eye and head movements, and as the amplitude of the gaze shift increases so does the contribution from the head. Perhaps under natural conditions outside of the scanner where head movements are allowed, the fairly large 16° saccades made by participants would contain a substantial mixture of head movements. Nonetheless, the fact that activity in the precuneus tracked learning under these circumstances may suggest that its involvement at the cortical level could facilitate the combined adaptation of gaze shifts of both the eye and the head. Although trials varied in the starting position of the eye in the orbit, they did so randomly across trials during the Preadapt and Adapt phases and therefore cannot account for these findings.

Similar to the precuneus, activity in the right anterior inferior parietal lobule (aIPL), specifically in the supramarginal gyrus, also predicted trial-to-trial reductions in saccade gain during adaptation. Unlike the precuneus, the magnitude of adaptation did not modulate its activity. Therefore, these two parietal areas likely make distinct contributions to saccade adaptation. The aIPL has been linked to a diverse set of visual, spatial, and motor functions, including both visual and motor adaptation (Chapman et al. 2010; Diedrichsen et al. 2005; Girgenrath et al. 2008). Damage to right aIPL causes hemineglect (Heilman et al. 2000; Mort et al. 2003), and its activity changes with attention state changes (Corbetta and Shulman 2002; Singh-Curry and Husain 2009). Some have argued that the aIPL plays an important role in motor attention, rather than visual or spatial attention, with the important distinction that attention is directed toward components of an effector in preparation for action rather than toward the features of external cues (Curtis and Connolly 2008; Rushworth et al. 2001a, 2001b). Such attention signals may be important for adaptive processes whether or not they impact the overall rate or degree of adaptation.

Adaptation begins when a motor error is detected. To study the mechanisms that maintain the calibration between the visual and motor systems, we artificially induced motor errors with intrasaccadic displacements of the target. We found that a number of cerebral and cerebellar areas tracked the size of saccade errors during the Adapt phase (Fig. 5). We found two clusters in the cerebellum whose activity tracked the size of saccade errors. These were surprisingly not in the oculomotor vermis but in left lobule V and right lobule VI. One previous fMRI study designed to identify regions of the cerebellum sensitive to saccade error reported that errors near what our participants experienced (~2°) were associated with greater cerebellar activity in lobule VI than larger (~5°) errors (Liem et al. 2013; see also Schlerf et al. 2012). During arm reaches to visual targets that are displaced during the reach, targeting errors activate portions of the posterior parietal cortex similar (Diedrichsen et al. 2005) to what we observed during saccades to displaced targets. This may indicate that the process of monitoring the consequences of motor error is not specific to the effector adapting. The literature is not consistent here, however, as reaching errors induced by prism glasses activate a different part of the intraparietal sulcus (Luauté et al. 2009) compared with what we found with saccades, indicating that there may indeed be some effector specificity.

Unlike Diedrichsen et al. (2005) and Luauté et al. (2009), we also find that in both the dorsolateral premotor and dorsomedial supplementary motor portions of frontal cortex, activity tracks the size of the saccade error. The areas where we found that errors are encoded, the superior precentral sulcus and paracentral sulcus, are thought to be the human homologs of macaque oculomotor areas frontal eye field and supplementary eye field, respectively (Curtis and Connolly 2008; Curtis and D'Esposito 2003; Miller et al. 2005). Therefore, the representation of error appears to be distributed in frontal and parietal cortex. Blurton et al. (2012) reported that activity in the dorsomedial frontal cortex decreased during saccade adaptation proportionally to the amount of adaptation, suggesting that it was an important area for oculomotor learning. However, the change in amplitude of saccade errors across learning, and the fact that such change would result in the smallest errors in participants with the greatest amount of adaptation, suggests that their effects could be driven by error processing and not learning. When we avoided that potential confound, we found that the dorsomedial frontal cortex tracks saccade errors and not adaptation per se. Similarly, the changes in activity in the temporo-parietal junction during saccade adaptation reported by Gerardin et al. (2012) may be driven by the difference in the visual target on the retina and current eye position following saccade errors. We find no evidence of learning-related signals in that area but do identify a small area nearby that does track saccade error.

Interestingly, in our task we always adapted leftward saccades, and since we used a backward step, the target error was always toward the right visual hemifield. Perhaps this explains the laterality of our findings. In frontal cortex, we find saccade error representations in the right superior precentral sulcus and paracentral sulcus, in the hemisphere contralateral to the saccade direction. In the parietal cortex, we find error representations in the left intraparietal and parietal-occipital sulcus, in the hemisphere contralateral to the retinal position of the visual saccade target. Indeed, neurons in the right premotor cortex of the macaque track the errors in the left arm while reaching (Inoue et al. 2016), consistent with our observations. Moreover, electrical stimulation of the left SC just after the saccade can introduce an error signal that drives adaptation, causing a gain decrease for leftward saccades (Kaku et al. 2009; Kojima et al. 2007; Soetedjo et al. 2009). It is plausible that the lateral parietal areas, which are connected with the SC, could also represent the contralateral visual error. Thus the visual and motor aspects of error might be differentially represented in the parietal and frontal cortex, possibly in different coordinate frames for vision and action.

These results have implications for theories of saccade adaptation if we consider the several subcomponents of sensorimotor adaptation within the control theory of motor learning (Shadmehr et al. 2010). Control of the eyes may involve an internal model that alters motor commands based on a feedforward model shaped by previous motor errors. In this framework, the feedforward model computes the predicted sensory consequences of saccades. Errors arise when the sensory con-

sequence of a movement mismatches the predicted consequence (Miall and Wolpert 1996). The cerebellum is thought to house neurons that act as a forward model that computes sensory prediction errors (Popa et al. 2016; Shadmehr et al. 2010; Sokolov et al. 2017; Streng et al. 2017). Our results provide additional support in the following ways. We found that activity in the oculomotor vermis increased during the adaptation of ipsiversive saccades, and the strength of this effect was proportional to the strength of adaptation within the learner. We did not observe learning-related activity during the later blocks of that Adapt phase (A2 and A3), when very little gain changes were observed in our participants, and we did not observe significant changes that predicted trial-to-trial gain changes across the entire Adapt phase. Moreover, the contribution of the cerebellum to saccade learning is unrelated to corrective saccades that could be used as a motor teaching signal and unrelated to the size of the saccade error during adaptation. Setting aside obvious issues related to the sensitivity of our measurements, we take the oculomotor vermis findings at face value. Doing so, we conclude that if the cerebellum acts as a forward model, it only adapted during the very first block of the Adapt phase (A1) and did so only in individuals who showed behavioral evidence of learning. Our modification of the classic double-step saccade adaptation experiment allowed us to rule out that the metrics of corrective saccades drove our measurements of learning. The mechanisms, whether visual feedback (Becker and Fuchs 1969; Tian et al. 2013) or extraretinal in nature (Collins and Wallman 2012; Weber and Daroff 1972), that prepare corrective saccades operate not only after the end of but also simultaneously with the preparation of primary saccades. If corrective saccades adapt along with primary saccades, the patterns of fMRI activation that we measured could be influenced by these adaptive mechanisms as well. However, the most parsimonious explanation is simply that our results are driven by the mechanisms that adapt primary saccades.

In the dorsomedial precuneus, we found increased activity during the adaptation of contraversive saccades, and again the strength of this effect was proportional to the strength of adaptation within the learner. Here, however, we did observe learning-related activity that predicted trial-to-trial gain changes throughout the Adapt phase, when one could argue it had very little effect on the overall reduction in measured saccade gain. Given that the position of the eye in the orbit is encoded by the neurons in a putatively homologous area in the macaque (Thier and Andersen 1998), we can speculate that it could help compute an inverse model of saccade control. To compute the saccade command, an inverse model needs to know the starting position of the eye. We may have potentiated this area with the use of multiple eye positions during our task, although this was not intended. Perhaps during the Adapt phase, saccade errors initiated updates to an inverse model encoded in the precuneus. Indeed, macaque area MP (aka 7m) shows strong spatially tuned postsaccade responses that are modulated by the current position of the eyes (Raffi et al. 2007). These quantities would be useful for computing inverse models of saccade control and adaptation. Optimal calibration of visually guided movements might depend on a control system that utilizes cooperating, but not necessarily synchronized, forward and inverse models of motor control (Aprasoff and Donchin 2012; Chen-Harris et al. 2008).

ACKNOWLEDGMENTS

We thank Josh Wallman for aid in piloting the experimental modification to the adaptation task. We thank New York University's Center for Brain Imaging for technical support.

GRANTS

This research was supported by the National Eye Institute (R01 EY-016407 to C. E. Curtis) and Fonds de Recherche Santé Québec (Graduate Research Fellowship Program to J. R. Fuller).

DISCLOSURES

No conflicts of interest, financial or otherwise, are declared by the authors.

AUTHOR CONTRIBUTIONS

R.S. and C.E.C. conceived and designed research; R.S. and C.E.C. performed experiments; A.G., J.R.F., R.S., and C.E.C. analyzed data; A.G. and C.E.C. interpreted results of experiments; A.G. and C.E.C. prepared figures; A.G., J.R.F., and C.E.C. drafted manuscript; A.G., J.R.F., and C.E.C. edited and revised manuscript; A.G., J.R.F., R.S., and C.E.C. approved final version of manuscript.

REFERENCES

Alahyane N, Fonteille V, Urquizar C, Salemme R, Nighoghossian N, Pelisson D, Tilikete C. Separate neural substrates in the human cerebellum for sensory-motor adaptation of reactive and of scanning voluntary saccades. *Cerebellum* 7: 595–601, 2008. doi:10.1007/s12311-008-0065-5.

Alahyane N, Salemme R, Urquizar C, Cotti J, Guillaume A, Vercher JL, Pélisson D. Oculomotor plasticity: are mechanisms of adaptation for reactive and voluntary saccades separate? *Brain Res* 1135: 107–121, 2007. doi:10.1016/j.brainres.2006.11.077.

Aprasoff J, Donchin O. Correlations in state space can cause sub-optimal adaptation of optimal feedback control models. *J Comput Neurosci* 32: 297–307, 2012. doi:10.1007/s10827-011-0350-z.

Barash S, Melikyan A, Sivakov A, Zhang M, Glickstein M, Thier P. Saccadic dysmetria and adaptation after lesions of the cerebellar cortex. *J Neurosci* 19: 10931–10939, 1999. doi:10.1523/JNEUROSCI.19-24-10931.1999.

Becker W, Fuchs AF. Further properties of the human saccadic system: eye movements and correction saccades with and without visual fixation points. *Vision Res* 9: 1247–1258, 1969. doi:10.1016/0042-6989(69)90112-6.

Berman RA, Colby CL, Genovese CR, Voyvodic JT, Luna B, Thulborn KR, Sweeney JA. Cortical networks subserving pursuit and saccadic eye movements in humans: an FMRI study. *Hum Brain Mapp* 8: 209–225, 1999. doi:10.1002/(SICI)1097-0193(1999)8:4<209::AID-HBM5>3.0.CO;2-0.

Blurton SP, Raabe M, Greenlee MW. Differential cortical activation during saccadic adaptation. *J Neurophysiol* 107: 1738–1747, 2012. doi:10.1152/jn.00682.2011.

Cavanna AE, Trimble MR. The precuneus: a review of its functional anatomy and behavioural correlates. *Brain* 129: 564–583, 2006. doi:10.1093/brain/awl004.

Chapman HL, Eramudugolla R, Gavrilescu M, Strudwick MW, Loftus A, Cunnington R, Mattingley JB. Neural mechanisms underlying spatial realignment during adaptation to optical wedge prisms. *Neuropsychologia* 48: 2595–2601, 2010. doi:10.1016/j.neuropsychologia.2010.05.006.

Chen-Harris H, Joiner WM, Ethier V, Zee DS, Shadmehr R. Adaptive control of saccades via internal feedback. *J Neurosci* 28: 2804–2813, 2008. doi:10.1523/JNEUROSCI.5300-07.2008.

Collins T, Wallman J. The relative importance of retinal error and prediction in saccadic adaptation. *J Neurophysiol* 107: 3342–3348, 2012. doi:10.1152/jn.00746.2011.

Corbetta M, Shulman GL. Control of goal-directed and stimulus-driven attention in the brain. *Nat Rev Neurosci* 3: 201–215, 2002. doi:10.1038/nrn755.

Cotti J, Guillaume A, Alahyane N, Pelisson D, Vercher JL. Adaptation of voluntary saccades, but not of reactive saccades, transfers to hand pointing movements. *J Neurophysiol* 98: 602–612, 2007. doi:10.1152/jn.00293.2007.

Cotti J, Panouilleres M, Munoz DP, Vercher JL, Pélisson D, Guillaume A. Adaptation of reactive and voluntary saccades: different patterns of adap-

tation revealed in the antisaccade task. *J Physiol* 587: 127–138, 2009. doi:10.1113/jphysiol.2008.159459.

Cox RW. AFNI: software for analysis and visualization of functional magnetic resonance neuroimages. *Comput Biomed Res* 29: 162–173, 1996. doi:10.1006/cbmr.1996.0014.

Curtis CE, Connolly JD. Saccade preparation signals in the human frontal and parietal cortices. *J Neurophysiol* 99: 133–145, 2008. doi:10.1152/jn.00899.2007.

Curtis CE, D'Esposito M. Persistent activity in the prefrontal cortex during working memory. *Trends Cogn Sci* 7: 415–423, 2003. doi:10.1016/S1364-6613(03)00197-9.

Desmurget M, Pélisson D, Grethe JS, Alexander GE, Urquizar C, Prablanc C, Grafton ST. Functional adaptation of reactive saccades in humans: a PET study. *Exp Brain Res* 132: 243–259, 2000. doi:10.1007/s002210000342.

Desmurget M, Pélisson D, Urquizar C, Prablanc C, Alexander GE, Grafton ST. Functional anatomy of saccadic adaptation in humans. *Nat Neurosci* 1: 524–528, 1998. [Erratum in *Nat Neurosci* 1: 743, 1998.] doi:10.1038/2241.

Diedrichsen J. A spatially unbiased atlas template of the human cerebellum. *Neuroimage* 33: 127–138, 2006. doi:10.1016/j.neuroimage.2006.05.056.

Diedrichsen J, Hashambhoy Y, Rane T, Shadmehr R. Neural correlates of reach errors. *J Neurosci* 25: 9919–9931, 2005. doi:10.1523/JNEUROSCI.1874-05.2005.

Fujikado T, Noda H. Saccadic eye movements evoked by microstimulation of lobule VII of the cerebellar vermis of macaque monkeys. *J Physiol* 394: 573–594, 1987. doi:10.1113/jphysiol.1987.sp016885.

Gerardin P, Miquée A, Urquizar C, Pélisson D. Functional activation of the cerebral cortex related to sensorimotor adaptation of reactive and voluntary saccades. *Neuroimage* 61: 1100–1112, 2012. doi:10.1016/j.neuroimage.2012.03.037.

Girgenrath M, Bock O, Seitz RJ. An fMRI study of brain activation in a visual adaptation task: activation limited to sensory guidance. *Exp Brain Res* 184: 561–569, 2008. doi:10.1007/s00221-007-1124-8.

Grosbras MH, Laird AR, Paus T. Cortical regions involved in eye movements, shifts of attention, and gaze perception. *Hum Brain Mapp* 25: 140–154, 2005. doi:10.1002/hbm.20145.

Haith AM, Krakauer JW. Model-based and model-free mechanisms of human motor learning. *Adv Exp Med Biol* 782: 1–21, 2013. doi:10.1007/978-1-4614-5465-6_1.

Havermann K, Lappe M. The influence of the consistency of postsaccadic visual errors on saccadic adaptation. *J Neurophysiol* 103: 3302–3310, 2010. doi:10.1152/jn.00970.2009.

Heilman KM, Valenstein E, Watson RT. Neglect and related disorders. *Semin Neurol* 20: 463–470, 2000. doi:10.1055/s-2000-13179.

Herman JP, Blangero A, Madelain L, Khan A, Harwood MR. Saccade adaptation as a model of flexible and general motor learning. *Exp Eye Res* 114: 6–15, 2013. doi:10.1016/j.exer.2013.04.001.

Hopp JJ, Fuchs AF. The characteristics and neuronal substrate of saccadic eye movement plasticity. *Prog Neurobiol* 72: 27–53, 2004. doi:10.1016/j.pneurobio.2003.12.002.

Inoue M, Uchimura M, Kitazawa S. Error signals in motor cortices drive adaptation in reaching. *Neuron* 90: 1114–1126, 2016. doi:10.1016/j.neuron.2016.04.029.

Jenkinson N, Miall RC. Disruption of saccadic adaptation with repetitive transcranial magnetic stimulation of the posterior cerebellum in humans. *Cerebellum* 9: 548–555, 2010. doi:10.1007/s12311-010-0193-6.

Kaku Y, Yoshida K, Iwamoto Y. Learning signals from the superior colliculus for adaptation of saccadic eye movements in the monkey. *J Neurosci* 29: 5266–5275, 2009. doi:10.1523/JNEUROSCI.0661-09.2009.

Kojima Y, Yoshida K, Iwamoto Y. Microstimulation of the midbrain tegmentum creates learning signals for saccade adaptation. *J Neurosci* 27: 3759–3767, 2007. doi:10.1523/JNEUROSCI.4958-06.2007.

Krakauer JW, Mazzoni P. Human sensorimotor learning: adaptation, skill, and beyond. *Curr Opin Neurobiol* 21: 636–644, 2011. doi:10.1016/j.conb.2011.06.012.

Kravitz DJ, Saleem KS, Baker CI, Mishkin M. A new neural framework for visuospatial processing. *Nat Rev Neurosci* 12: 217–230, 2011. doi:10.1038/nrn3008.

Leichnetz GR. Connections of the medial posterior parietal cortex (area 7m) in the monkey. *Anat Rec* 263: 215–236, 2001. doi:10.1002/ar.1082.

Liem EI, Frens MA, Smits M, van der Geest JN. Cerebellar activation related to saccadic inaccuracies. *Cerebellum* 12: 224–235, 2013. doi:10.1007/s12311-012-0417-z.

Luauté J, Schwartz S, Rossetti Y, Spiridon M, Rode G, Boisson D, Vuilleumier P. Dynamic changes in brain activity during prism adaptation. *J Neurosci* 29: 169–178, 2009. doi:10.1523/JNEUROSCI.3054-08.2009.

Lynch JC, Tian JR. Cortico-cortical networks and cortico-subcortical loops for the higher control of eye movements. *Prog Brain Res* 151: 461–501, 2006. doi:10.1016/S0079-6123(05)51015-X.

Margulies DS, Vincent JL, Kelly C, Lohmann G, Uddin LQ, Biswal BB, Villringer A, Castellanos FX, Milham MP, Petrides M. Precuneus shares intrinsic functional architecture in humans and monkeys. *Proc Natl Acad Sci USA* 106: 20069–20074, 2009. doi:10.1073/pnas.0905314106.

McLaughlin S. Parametric adjustment in saccadic eye movements. *Atten Percept Psychophys* 2: 359–362, 1967. doi:10.3758/BF03210071.

Miall RC, Wolpert DM. Forward models for physiological motor control. *Neural Netw* 9: 1265–1279, 1996. doi:10.1016/S0893-6080(96)00035-4.

Miller LM, Sun FT, Curtis CE, D'Esposito M. Functional interactions between oculomotor regions during prosaccades and antisaccades. *Hum Brain Mapp* 26: 119–127, 2005. doi:10.1002/hbm.20146.

Mort DJ, Malhotra P, Mannan SK, Rorden C, Pambakian A, Kennard C, Husain M. The anatomy of visual neglect. *Brain* 126: 1986–1997, 2003. doi:10.1093/brain/awg200.

Müri RM. MRI and fMRI analysis of oculomotor function. *Prog Brain Res* 151: 503–526, 2006. doi:10.1016/S0079-6123(05)51016-1.

Noto CT, Robinson FR. Visual error is the stimulus for saccade gain adaptation. *Brain Res Cogn Brain Res* 12: 301–305, 2001. doi:10.1016/S0926-6410(01)00062-3.

Optican LM, Robinson DA. Cerebellar-dependent adaptive control of primate saccadic system. *J Neurophysiol* 44: 1058–1076, 1980. doi:10.1152/jn.1980.44.6.1058.

Pandya DN, Seltzer B. Intrinsic connections and architectonics of posterior parietal cortex in the rhesus monkey. *J Comp Neurol* 204: 196–210, 1982. doi:10.1002/cne.902040208.

Panouillères M, Alahyane N, Urquizar C, Salemme R, Nighoghossian N, Gaymard B, Tilikete C, Pélisson D. Effects of structural and functional cerebellar lesions on sensorimotor adaptation of saccades. *Exp Brain Res* 231: 1–11, 2013. doi:10.1007/s00221-013-3662-6.

Panouillères M, Neggers SF, Gutteling TP, Salemme R, van der Stigchel S, van der Geest JN, Frens MA, Pélisson D. Transcranial magnetic stimulation and motor plasticity in human lateral cerebellum: dual effect on saccadic adaptation. *Hum Brain Mapp* 33: 1512–1525, 2012. doi:10.1002/hbm.21301.

Pélisson D, Alahyane N, Panouillères M, Tilikete C. Sensorimotor adaptation of saccadic eye movements. *Neurosci Biobehav Rev* 34: 1103–1120, 2010. doi:10.1016/j.neubiorev.2009.12.010.

Popa LS, Streng ML, Hewitt AL, Ebner TJ. The errors of our ways: understanding error representations in cerebellar-dependent motor learning. *Cerebellum* 15: 93–103, 2016. doi:10.1007/s12311-015-0685-5.

Prsa M, Thier P. The role of the cerebellum in saccadic adaptation as a window into neural mechanisms of motor learning. *Eur J Neurosci* 33: 2114–2128, 2011. doi:10.1111/j.1460-9568.2011.07693.x.

Raffi M, Squatrito S, Maioli MG. Gaze and smooth pursuit signals interact in parietal area 7m of the behaving monkey. *Exp Brain Res* 182: 35–46, 2007. doi:10.1007/s00221-007-0967-3.

Robinson FR, Fuchs AF, Noto CT. Cerebellar influences on saccade plasticity. *Ann NY Acad Sci* 956: 155–163, 2002. doi:10.1111/j.1749-6632.2002.tb02816.x.

Rushworth MF, Krams M, Passingham RE. The attentional role of the left parietal cortex: the distinct lateralization and localization of motor attention in the human brain. *J Cogn Neurosci* 13: 698–710, 2001a. doi:10.1162/089892901750363244.

Rushworth MF, Paus T, Sipila PK. Attention systems and the organization of the human parietal cortex. *J Neurosci* 21: 5262–5271, 2001b. doi:10.1523/JNEUROSCI.21-14-05262.2001.

Schlerf J, Ivry RB, Diedrichsen J. Encoding of sensory prediction errors in the human cerebellum. *J Neurosci* 32: 4913–4922, 2012. doi:10.1523/JNEUROSCI.4504-11.2012.

Schmahmann JD, Doyon J, Toga A, Evans A, Petrides M. *MRI Atlas of the Human Cerebellum*. San Diego, CA: Academic, 2000.

Seidler RD, Purushotham A, Kim SG, Uğurbil K, Willingham D, Ashe J. Cerebellum activation associated with performance change but not motor learning. *Science* 296: 2043–2046, 2002. doi:10.1126/science.1068524.

Shadmehr R, Krakauer JW. A computational neuroanatomy for motor control. *Exp Brain Res* 185: 359–381, 2008. doi:10.1007/s00221-008-1280-5.

Shadmehr R, Smith MA, Krakauer JW. Error correction, sensory prediction, and adaptation in motor control. *Annu Rev Neurosci* 33: 89–108, 2010. doi:10.1146/annurev-neuro-060909-153135.

Singh-Curry V, Husain M. The functional role of the inferior parietal lobe in the dorsal and ventral stream dichotomy. *Neuropsychologia* 47: 1434–1448, 2009. doi:10.1016/j.neuropsychologia.2008.11.033.

Soetedjo R, Fuchs AF, Kojima Y. Subthreshold activation of the superior colliculus drives saccade motor learning. *J Neurosci* 29: 15213–15222, 2009. doi:10.1523/JNEUROSCI.4296-09.2009.

Sokolov AA, Miall RC, Ivry RB. The cerebellum: adaptive prediction for movement and cognition. *Trends Cogn Sci* 21: 313–332, 2017. doi:10.1016/j.tics.2017.02.005.

Srimal R, Diedrichsen J, Ryklin EB, Curtis CE. Obligatory adaptation of saccade gains. *J Neurophysiol* 99: 1554–1558, 2008. doi:10.1152/jn.01024.2007.

Straube A, Deubel H, Ditterich J, Eggert T. Cerebellar lesions impair rapid saccade amplitude adaptation. *Neurology* 57: 2105–2108, 2001. doi:10.1212/WNL.57.11.2105.

Streng ML, Popa LS, Ebner TJ. Climbing fibers control purkinje cell representations of behavior. *J Neurosci* 37: 1997–2009, 2017. doi:10.1523/JNEUROSCI.3163-16.2017.

Takagi M, Tamargo R, Zee DS. Effects of lesions of the cerebellar oculomotor vermis on eye movements in primate: binocular control. *Prog Brain Res* 142: 19–33, 2003. doi:10.1016/S0079-6123(03)42004-9.

Thier P, Andersen RA. Electrical microstimulation distinguishes distinct saccade-related areas in the posterior parietal cortex. *J Neurophysiol* 80: 1713–1735, 1998. doi:10.1152/jn.1998.80.4.1713.

Tian J, Ying HS, Zee DS. Revisiting corrective saccades: role of visual feedback. *Vision Res* 89: 54–64, 2013. doi:10.1016/j.visres.2013.07.012.

Tin C, Poon CS. Internal models in sensorimotor integration: perspectives from adaptive control theory. *J Neural Eng* 2: S147–S163, 2005. doi:10.1088/1741-2560/2/3/S01.

Tse PU, Baumgartner FJ, Greenlee MW. Event-related functional MRI of cortical activity evoked by microsaccades, small visually-guided saccades, and eyeblinks in human visual cortex. *Neuroimage* 49: 805–816, 2010. doi:10.1016/j.neuroimage.2009.07.052.

Tseng YW, Diedrichsen J, Krakauer JW, Shadmehr R, Bastian AJ. Sensory prediction errors drive cerebellum-dependent adaptation of reaching. *J Neurophysiol* 98: 54–62, 2007. doi:10.1152/jn.00266.2007.

Waespe W, Baumgartner R. Enduring dysmetria and impaired gain adaptivity of saccadic eye movements in Wallenberg's lateral medullary syndrome. *Brain* 115: 1125–1146, 1992. doi:10.1093/brain/115.4.1125.

Wallman J, Fuchs AF. Saccadic gain modification: visual error drives motor adaptation. *J Neurophysiol* 80: 2405–2416, 1998. doi:10.1152/jn.1998.80.5.2405.

Weber RB, Daroff RB. Corrective movements following refixation saccades: type and control system analysis. *Vision Res* 12: 467–475, 1972. doi:10.1016/0042-6989(72)90090-9.

Wolpert DM, Diedrichsen J, Flanagan JR. Principles of sensorimotor learning. *Nat Rev Neurosci* 12: 739–751, 2011. doi:10.1038/nrn3112.

Wolpert DM, Flanagan JR. Computations underlying sensorimotor learning. *Curr Opin Neurobiol* 37: 7–11, 2016. doi:10.1016/j.conb.2015.12.003.

Wong AL, Shelhamer M. Sensorimotor adaptation error signals are derived from realistic predictions of movement outcomes. *J Neurophysiol* 105: 1130–1140, 2011. doi:10.1152/jn.00394.2010.

Yamada J, Noda H. Afferent and efferent connections of the oculomotor cerebellar vermis in the macaque monkey. *J Comp Neurol* 265: 224–241, 1987. doi:10.1002/cne.902650207.